Journal of Power Sources 195 (2010) 6001–6007

Contents lists available at ScienceDirect

Journal of Power Sources

journal homepage: www.elsevier.com/locate/jpowsour

Development of a method to estimate the lifespan of proton exchange membrane fuel cell using electrochemical impedance spectroscopy

Ju-hyung Lee [a], Jong-Hak Lee [a], Woojin Choi [a,*], Kyung-Won Park [b], Hee-Young Sun [c], Jae-Hyuk Oh [d]

[a] Department of Electrical Engineering, Soongsil University, 1-1 Sangdo-dong, Dongjak-gu, Seoul 156-743, Republic of Korea
[b] Department of Chemical/Environmental Engineering, Soongsil University, 1-1 Sangdo-dong, Dongjak-gu, Seoul 156-743, Republic of Korea
[c] Samsung Advanced Institute of Technology, Mt. 14-1, Nongseo-dong, Giheung-gu, Yongin-si, Gyeonggi-do 446-712, Republic of Korea
[d] Samsung Electronics, 416 Maetan-dong, Youngtong-gu, Suwon-si, Gyeonggi-do 443-370, Republic of Korea

ARTICLE INFO

Article history:
Received 30 September 2009
Received in revised form 17 February 2010
Accepted 19 February 2010
Available online 12 March 2010

Keywords:
Fuel cell
Electrochemical impedance spectroscopy
Parameter change
Time constant
State of health
Lifespan

ABSTRACT

This paper proposes a new method for estimating the state and lifespan of fuel cells in operation by fuel cell equivalent impedance modeling by electrochemical impedance spectroscopy (EIS) and observing degradation. The performance change of fuel cells takes place in the form of changes in each parameter value comprising an equivalent AC impedance circuit; monitoring such changes allows for the prediction of the state and lifespan of a fuel cell. In the experiments, the AC impedance of high-temperature proton exchange membrane (PEM) fuel cells was measured at constant time intervals during their continuous operation for over 2200 h. The expression for the lifespan of a fuel cell was deduced by curve fitting the changes in each parameter to a polynomial. Electric double layer capacitance and charge transfer resistance, which show the reduction reaction of the cathode, were used as major parameters for judging the degradation; a method of using time constants is proposed to more accurately estimate the degree of degradation. In addition, an algorithm that can evaluate the soundness and lifespan of a fuel cell is proposed; it compares the measured time constant of the fuel cell being tested with that of average lifespan fuel cell.

1. Introduction

The two major factors influencing fuel cell commercialization are the price and reliability of the fuel cell stack. The price can be reduced by replacing expensive components such as platinum catalysts with innovative materials, simplifying the system, automating membrane electrode assembly (MEA) production, and mass production [1,2]. On the other hand, reliability depends greatly on the condition of technical improvements, and it is also affected by the production technique and quality management. The degradation of performance of fuel cells in operation occurs due to various causes: humidity and temperature cycles, catalyst poisoning, performance degradation of support, starting and stopping, load cycle, idling, etc. This directly affects the system reliability. Therefore, predicting a potential failure through an accurate evaluation of the state of fuel cells in operation can dramatically reduce the service costs due to abrupt failure and, ultimately, significantly improve system reliability.

A number of studies on fuel cell performance evaluation and lifespan estimation have been conducted, and various methods for fuel cell performance evaluation have been proposed [3–5]. Ciureanu and Roberge proposed a method for determining stack performance changes from the changes in the humidifying temperature and air flow; they used the parameters included in the thin film flooded-agglomerate model and Tafel expressions, which modeled gas diffusion electrode changes according to the operating conditions. They used electrochemical impedance spectroscopy (EIS) to obtain the value of the cathode charge transfer resistance required for performance evaluation [3]. Merida et al. proposed a method for determining the fuel cell performance from the moisture content change. They selected the ratio of the fuel cell impedance value and the standard fuel cell impedance value as the performance determining parameter; using the fact that such a ratio differs at specific frequency ranges depending on performance changes, they proposed a method for determining dehydration and flooding [4]. Laffly et al. measured the impedance of a fuel cell operating for approximately 1000 h, by EIS; after monitoring, they determined the equivalent impedance circuit parameter change and analyzed the factors causing the parameter change [5]. The analysis results showed that fuel cell degradation occurs due to various causes; once a fuel cell in operation enters the degradation stage, the degree of progress can be determined by the change in the

* Corresponding author. Tel.: +82 2 820 0652; fax: +82 2 817 7961.
E-mail addresses: t_tcrying@hotmail.com (J.-h. Lee), jonghak123@hotmail.com (J.-H. Lee), cwj777@ssu.ac.kr (W. Choi), kwpark@ssu.ac.kr (K.-W. Park), hysun@samsung.com (H.-Y. Sun), jae.oh@samsung.com (J.-H. Oh).

0378-7753/$ – see front matter © 2010 Elsevier B.V. All rights reserved.
doi:10.1016/j.jpowsour.2010.02.054

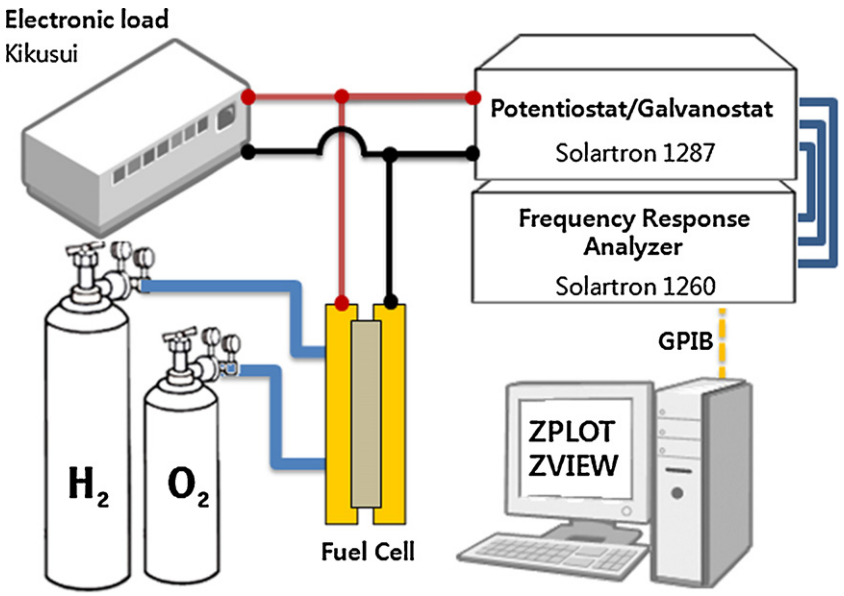

Fig. 1. Experimental apparatus used for EIS measurement of high-temperature PEM fuel cell.

fuel cell equivalent impedance parameter. Therefore, the fuel cell performance and remaining lifespan can be sensed by monitoring the impedance change.

2. Experimental

In the experiments, a polybenzoxazine-based membrane was used for the MEA evaluation of catalysts; the amount of phosphoric acid in the membrane was controlled by immersing a dry membrane in phosphoric acid at 80 °C for a few hours. The cathode catalyst layer was composed of PtCo–CeOx or PtCo supported on Ketzen black and polyvinylidene fluoride (PVDF). The anode catalyst layer was composed of a carbon-supported PtRu alloy, from Tanaka Kikinzoku Kogyo, and PVDF. The Pt loadings of the cathode and anode were approximately 1.6 and 1.0 mg cm^{-2}, respectively. Dry hydrogen and dry air were used for the anode and cathode, respectively, during the cell operation at 150 °C. The effective dimensions of the electrode in the MEA were 2.8 cm × 2.8 cm [6].

Hydrogen was supplied to the anode of the cell at a pressure of 0.3 MPa with no humidification and at a flow rate of 100 ccm at 99.99% purity; air was supplied to the cathode of the cell under moisture-free conditions at a pressure of 0.3 MPa and a flow rate of 250 ccm. The rates of utilization of hydrogen and oxygen were 26% and 20%, respectively.

The composition of the AC impedance measurement system used in the experiments is shown in Fig. 1. The system is arranged such that Kikusui DC electronic load and a Solartron 1287 potentiostat–galvanostat are connected in parallel to the cell being tested; this enables the impedance to be measured in any area of operation of the fuel cell. A Solartron 1260 frequency response analyzer controls the potentiostat–galvanostat. To measure the impedance at a desired operation point, fuel cell AC perturbations are induced by adjusting the Kikusui DC electronic load and DC operation current and operating Solartron 1287 in the galvanostat mode; through calculations using the perturbation current and measured response voltage, impedance can be calculated. The AC impedance was measured by taking 10 points per decade in the 0.01–10 kHz frequency ranges.

The electronic load and FRA were controlled by using the Zplot software installed in a personal computer (PC); the measured impedance data was transferred to the PC via GPIB, and curve fitting by the impedance model was done using Zview.

Fig. 2 shows a Nyquist plot of the AC impedance measured using EIS. In the 0.5–2 A region, the loss due to activation was dominant, and the slope of the voltage change was large; measurements were performed in steps of 0.5 A. In the region beyond that, AC impedance was measured by changing the DC operation point in steps of 1 A. The Nyquist plot indicates that the change in the size of the impedance semicircle diameter was the same as the change in the slope of the polarization curve [7]. In addition, the impedance of the anode had a very small trajectory due to the rapid hydrogen oxidation reaction, but the cathode impedance had a large trajectory due to the slow reduction reaction [8].

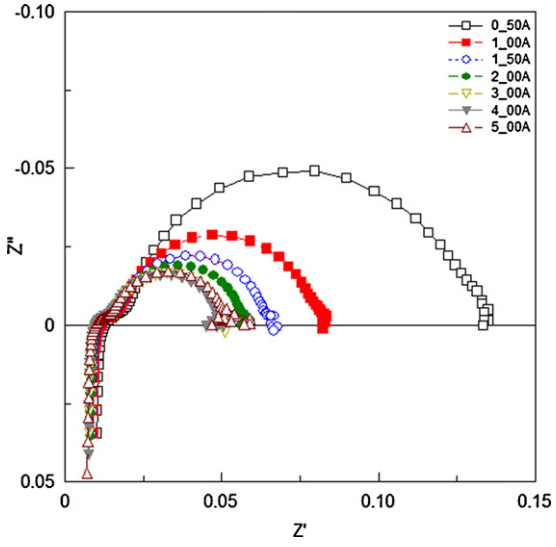

Fig. 2. Nyquist impedance plots of fuel cell measured at different operating points.

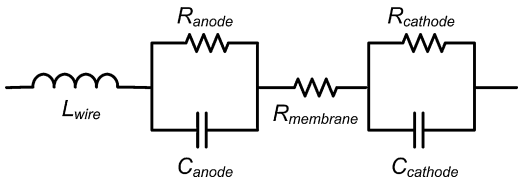

Fig. 3. Equivalent circuit model of PEM fuel cell used in curve fitting.

3. Results and discussion

3.1. High-temperature fuel cell equivalent circuit model and degradation phenomenon

There are various equivalent circuit models that can be used for the analysis of the AC impedance spectrum of fuel cells measured by EIS. These models can be applied differently depending on the measurement object, the operation point at which the impedance is measured, and the measured frequency region; the most widely used models clearly show the phenomenon being observed while reflecting the physical properties of the measurement object.

The general models of the equivalent impedance of fuel cells are composed of resistance components such as the ion resistance of electrolytes, electrical resistance of cell components, charge transfer resistance, electric double layer capacitance from ions densely distributed at the three-phase interface, Warburg impedance due to gas diffusion, and microscopic inductance components. Electric double layer capacitor, which is usually referred to as the constant phase element (CPE) due to the nonuniformity of the electrode surface, is often used as ZARC by forming parallel circuits with charge transfer resistance. When using a CPE in the equivalent circuit modeling of the fuel cell, more accurate fitting results can be obtained, but when the depression angle n approximates 1, a moderate fitting result may be obtained even if a capacitor is used [9,10].

In this study, the measured impedance was fitted to a curve, and the changes in the parameters were studied. Fig. 3 shows the equivalent circuit used, which has two R–C parallel circuits and a membrane resistance between them. This circuit can explain the two dominant reactions of a fuel cell – anode oxidation and cathode reduction – from the two semicircles on the Nyquist plot, which are obtained from the measured impedance of the fuel cell [11,12]. By expressing the fuel cell impedance in the equivalent circuit using two time constants the oxidation and reduction reaction rates can also be expressed using time constants. Since the maximum current of the cell is 7.84 A (1 A cm^{-2}), there was barely any mass transfer loss in the 1–5 A range; therefore, the Warburg impedance was not included in the equivalent circuit.

Fuel cell degradation occurs mostly in cathode catalysts due to various causes such as catalyst dissolution and precipitation, aging, catalyst particle movement, and carbon support corrosion [13,14]. Nanosized catalyst particles undergo condensation through dissolution and precipitation reactions to reduce surface energy; this decreases the three-phase interface area required for the reduction reaction, which degrades the fuel cell. The decrease in the electrochemical surface area leads to a decrease in the reduction reaction rate, which in turn results in an increase in the charge transfer resistance value. In addition, such a phenomenon also leads to the reduction of the electric double layer capacitance in the three-phase interface, which reduces the capacitance value. The continued condensation of catalyst particles can cause oxidation or corrosion of the carbon support layer; this weakens the attaching force of catalyst particles, which can cause the infiltration of catalyst particles into the membrane or electrode. This loss of catalysts causes the fuel cell performance to drop, which changes the fuel cell equivalent circuit parameter value [1,14,15].

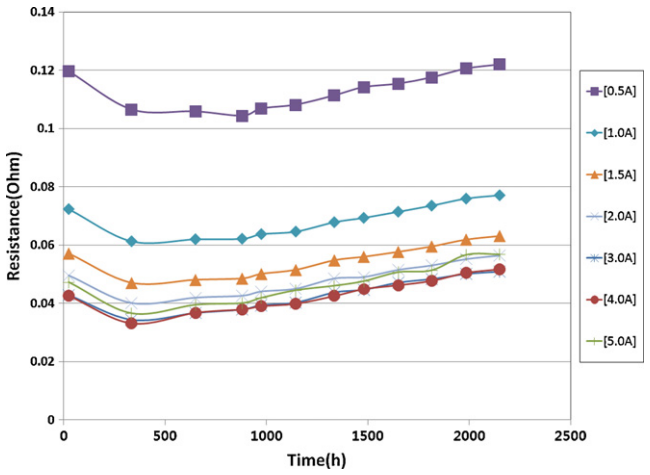

Fig. 4. Change in cathode charge transfer resistance during 2200 h of operation.

3.2. Fuel cell parameter monitoring

To observe the change in the equivalent impedance model parameters during the continuous operation of a high-temperature fuel cell, EIS experiments were repeated 12 times at 7 operation points at 168 h (7 days) intervals; the fuel cell was operated for 2200 h (around 90 days) under the conditions explained in Section 2, and the results were analyzed.

Figs. 4–8 show graphs of changes in each parameter with time obtained by curve fitting the measured fuel cell impedance spectrum to the equivalent circuit shown in Fig. 3. As shown in the graphs, the charge transfer resistance of each electrode and the membrane resistance dramatically decreased from the start of the operation to approximately 335 h, during which the electric double layer capacitance of each electrode increased. This period, where the performance improved for the initial operation after fuel cell production, is called the break-in period [16]. During this period, the fuel cell exhibits continuous performance improvement; afterwards, the performance no longer improves but begins to degrade.

The change in the impedance parameter for the cathode side that shows a clear semicircle in the Nyquist impedance plot is explained here. As shown in Figs. 4 and 5, the charge transfer resistance on the cathode side gradually increased, while the electric double layer capacitance on the cathode side gradually decreased. Both these phenomena occurred due to the reduction of the catalysis reaction rate and three-phase interface area. The nanoparticle

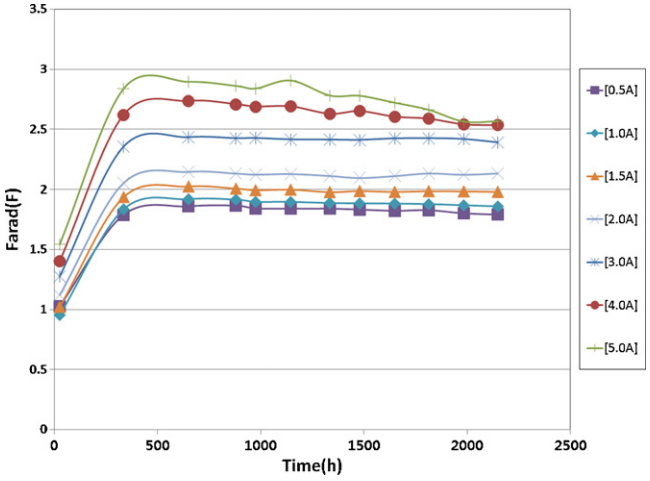

Fig. 5. Change in cathode double layer capacitance during 2200 h of operation.

Table 1
List of coefficients for curve-fitting expression of cathode charge transfer resistance.

Current [A]	$y_{modeled} = at^4 + bt^3 + ct^2 + dt + e$					Accuracy [%]
	a	*b*	*c*	*d*	*e*	
0.5	1.9E−14	−5.9E−11	9.7E−08	−6.8E−05	1.2E−01	98.7
1.0	4.3E−14	−1.0E−10	1.3E−07	−6.9E−05	7.4E−02	99.4
1.5	4.5E−14	−3.5E−11	7.1E−08	−5.1E−05	5.8E−02	99.0
2.0	4.3E−14	−3.4E−11	6.8E−08	−4.7E−05	5.0E−02	98.5
3.0	4.2E−14	−1.0E−10	1.2E−07	−5.8E−05	4.4E−02	99.3
4.0	6.2E−14	−1.4E−10	1.6E−07	−7.0E−05	4.4E−02	98.9
5.0	6.9E−14	−1.6E−10	1.8E−07	−8.0E−05	4.9E−02	98.6

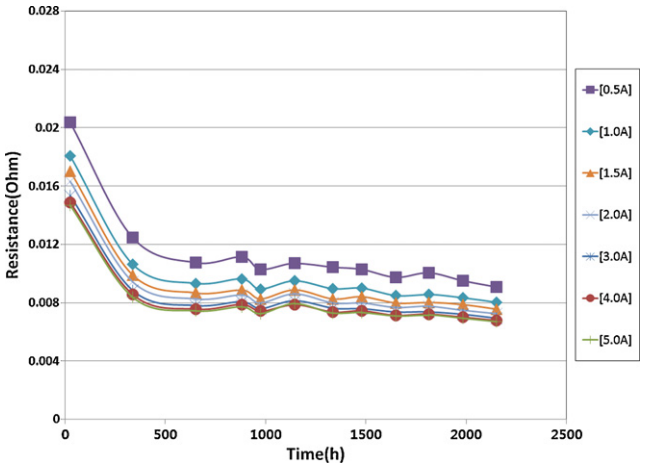

Fig. 6. Change in membrane resistance during 2200 h of operation.

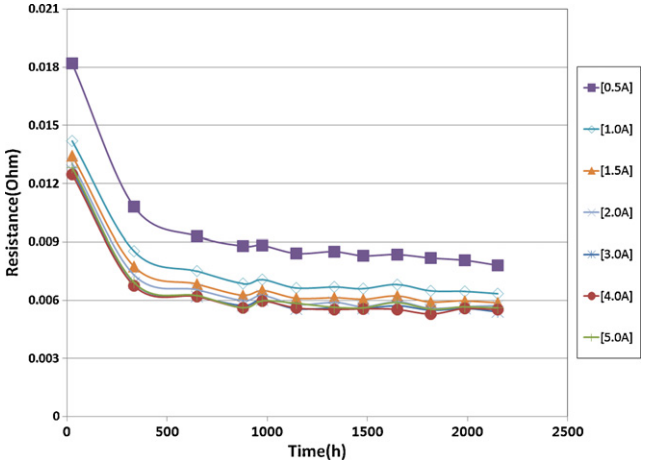

Fig. 7. Change in anode charge transfer resistance during 2200 h of operation.

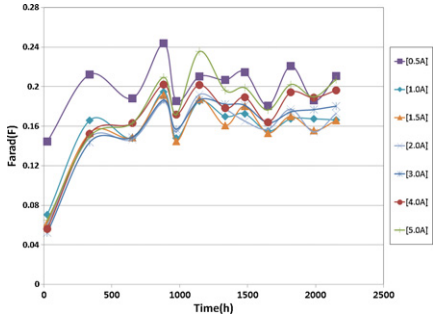

Fig. 8. Change in anode double layer capacitance during 2200 h of operation.

catalysts tend to aggregate due to their high specific surface energy, and this tendency becomes clearer under harsher operating conditions [14]. In addition, the collapse of the support slows down the electric charge transmission due to diffusion of the catalyst into the boundary surface of the electrode or electrolyte; this also affects the rate of the reduction reaction. Thus, the decrease in the catalysis activation area due to such phenomena degrades the cell performance, which increases the charge transfer resistance and decreases the electric double layer capacitance value in equivalent circuit impedance. In other words, as the aging of the cathode side continues, the rate of the reduction reaction is reduced.

As shown in Fig. 4, as the fuel cell experiences aging due to continuous operation, the parameters of the equivalent impedance model reflect the performance change due to degradation of cell components. Therefore, such parameter changes can be mathematically modeled using a function of time and the lifespan of fuel cell can be estimated.

To mathematically express the change in parameter with time, it is expressed by a polynomial expression obtained through the curve fitting. The coefficient of the polynomial expression can be calculated through linear regression analysis, and the accuracy of the curve fitting is calculated by using the coefficient of determination, as given by Eq. (1) [17].

$$R^2 = \frac{\sum (y_{measured} - \bar{y})^2 - \sum (y_{measured} - y_{modeled})^2}{\sum (y_{measured} - \bar{y})^2} \quad (1)$$

where $y_{measured}$ is the measured data, $\bar{y}$ is the mean of the measured data, and $y_{modeled}$ is the data from the model.

A fourth-order polynomial expression was used to model the change in the measured cathode charge transfer resistance with time. Table 1 shows the list of the coefficients for the fourth-order polynomial expression of curve fitting of cathode charge transfer resistance by time elapse and the curve fitting accuracies at the operating points. Differences exist among the operating points, but most of them showed over 98% accuracy. Fig. 5 and Table 2 show the waveforms of the changes in the electric double layer capacitance measured at multiple operation points, and the list of the coefficients and their accuracies. The results show an accuracy of over 96% for the entire range of operation. However, as mentioned previously, the reduction of catalysis performance due to fuel cell degradation not only increases the electric charge transfer resistance but also decreases the electric double layer capacitance; therefore, a more accurate expression can be obtained if it is deduced using a time constant – the product of two parameters – rather than using each parameter separately. Here, the time constant ultimately indicates the time ratio of the reduction reaction occurring in the cathode; it serves as an indicator of the reduction reaction occurring at the three-phase interface.

Fig. 9 and Table 3 show the waveforms of the changes in the cathode time constant with time, the product of the cathode charge transfer resistance and electric double layer capacitance, and the list of coefficients and their accuracies. As anticipated, as compared to curve fitting using either the cathode charge transfer resistance

Table 2
List of coefficients for curve-fitting expression of cathode double layer capacitance.

Current [A]	$y_{modeled} = at^4 + bt^3 + ct^2 + dt + e$					Accuracy [%]
	a	*b*	*c*	*d*	*e*	
0.5	−5.3E−13	2.8E−09	−5.1E−06	3.7E−03	9.5E−01	98.4
1.0	−6.1E−13	3.2E−09	−5.9E−06	4.3E−03	8.7E−01	98.4
1.5	−6.4E−13	3.4E−09	−6.2E−06	4.5E−03	9.3E−01	98.5
2.0	−6.4E−13	3.4E−09	−6.3E−06	4.6E−03	1.0E+00	98.5
3.0	−7.9E−13	4.1E−09	−7.4E−06	5.3E−03	1.2E+00	98.3
4.0	−8.2E−13	4.3E−09	−8.0E−06	5.9E−03	1.3E+00	98.1
5.0	−8.2E−13	4.3E−09	−8.2E−06	6.1E−03	1.4E+00	96.1

Table 3
List of coefficients for curve-fitting expression of cathode time constant and curve-fitting accuracy.

Current [A]	$y_{modeled} = at^4 + bt^3 + ct^2 + dt + e$					Accuracy [%]
	a	*b*	*c*	*d*	*e*	
0.5	−5.5E−14	2.8E−10	−4.8E−07	3.3E−04	1.2E−01	98.3
1.0	−3.5E−14	1.8E−10	−3.0E−07	2.2E−04	6.5E−02	99.3
1.5	−2.5E−14	1.3E−10	−2.1E−07	1.6E−04	5.5E−02	99.3
2.0	−2.0E−14	1.0E−10	−1.7E−07	1.3E−04	5.3E−02	99.6
3.0	−2.2E−14	1.0E−10	−1.7E−07	1.3E−04	5.2E−02	99.7
4.0	−1.6E−14	8.4E−11	−1.5E−07	1.3E−04	5.7E−02	99.6
5.0	−1.6E−14	8.4E−11	−1.5E−07	1.3E−04	7.0E−02	98.3

or electric double layer capacitance, the accuracy is over 99% for the entire range of operation; thus, measuring the impedance of the fuel cell in operation and monitoring the cathode time constant value can give a very accurate estimate for the state and lifespan of the fuel cell. Details of the estimation method are explained in the next section.

3.3. Fuel cell state evaluation and lifespan estimation method

Since the polynomial expression of the change in the cathode time constant almost exactly reflects the performance degradation of the fuel cell, it is reasonable to use it as the lifespan expression. In the experiments, the fuel cell was being operated at 3 A (0.38 A cm^{-2}) continuously and among the lifespan expressions at operation points in Table 3, the accuracy of it at 3 A is the best; thus, the lifespan is estimated using this lifespan expression.

The lifespan expression for the fuel cell performance as a polynomial includes both the break-in period, where the standard fuel cell performance improves, and the degradation period; thus, the change in the cathode time constant over the entire lifespan of fuel cell can be expressed numerically. This feature allows the lifespan to be estimated and the performance to be evaluated in the early stages of fuel cell operation and during the aging process. If the average lifespan expression deduced from multiple fuel cell data is the same as that given in Table 3, it can be used as a standard lifespan expression.

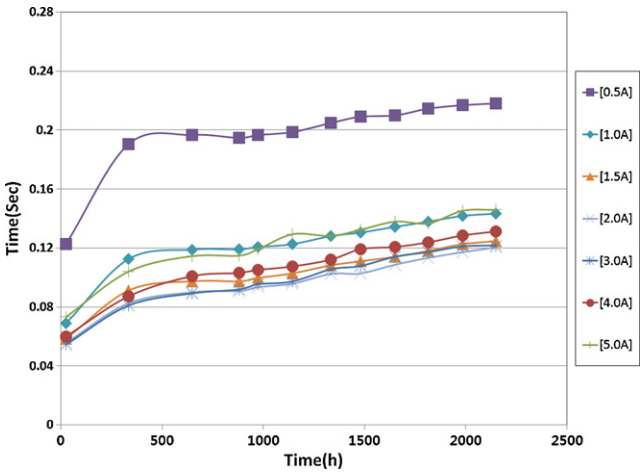

Fig. 9. Change in cathode time constant during 2200 h of operation.

To estimate the fuel cell soundness condition and lifespan using a standard lifespan expression, the standard cathode time constant ($\tau_{cathode\_standard}$) is calculated by substituting the cumulative operation time of the fuel cell under test into the lifespan expression for 3 A. The ratio of the cathode time constant ($P_K(t)$) measured at operation time t for the standard cathode time constant calculated above is expressed by Eq. (2); this expression can be used to evaluate the remaining life and state of the fuel cell. An evaluation of the fuel cell state and remaining life can be divided into the following three cases:

$$P_K(t) = \frac{\tau_{cathode}(t)}{\tau_{cathode\_standard}} \quad (2)$$

In the first case, the ratio of the two values ($P_K(t)$) is 1. In this case, the cell is determined to be sound, and the difference between the average lifespan (L_{avg}) deduced through experiments for multiple fuel cells, and the cumulative operation time t is calculated as the remaining lifespan, as given by Eq. (3). The calculation for the average lifespan of the fuel cell is explained in detail in the next section:

$$L_{rem} = L_{avg} - t \quad (3)$$

In the second case, the ratio is less than 1. In this case, the fuel cell degradation is less than the average degradation. Thus, the fuel cell is determined to be very sound, and the remaining life is calculated as the difference between the average lifespan divided by the ratio of the cathode time constant (P_K) and the cumulative operation time t, as given by Eq. (4):

$$L_{rem} = \frac{L_{avg}}{P_K(t)} - t \quad (4)$$

In the third case, the ratio is greater than 1. In this case, the fuel cell has degraded more severely than average and is thus determined to be unsound. The remaining life is calculated in the same way as the second case.

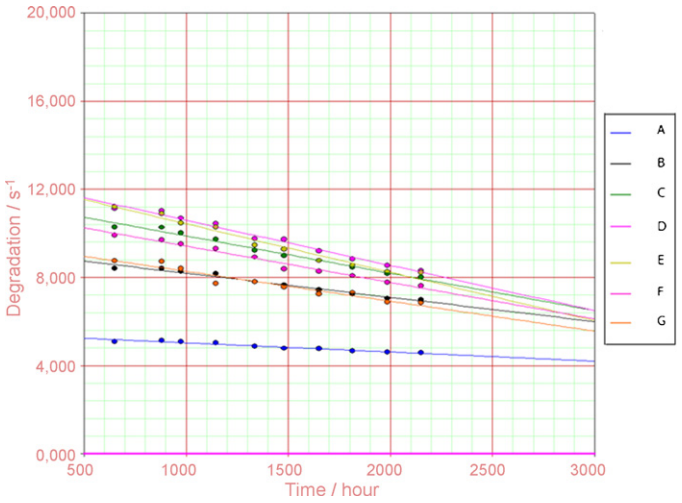

Fig. 10. Degradation plots of fuel cell obtained from virtually measured multiple fuel cell impedance.

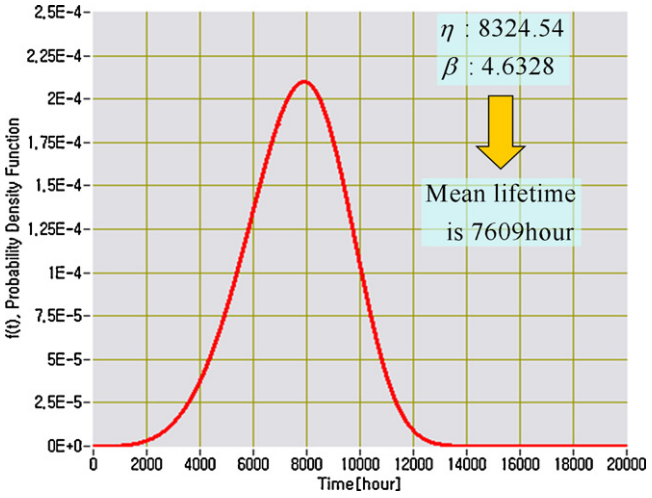

Fig. 11. Probability density function of fuel cell lifespan obtained from lifespan data of multiple fuel cells.

3.4. Fuel cell average lifespan calculation

The performance of a fuel cell is bound to degrade after the break-in period. The lifespan of a standard fuel cell can be calculated by modeling the degradation mathematically. In the waveforms of the changes in the cathode time constant with time in Fig. 9, the data of break-in period, during which the performance improves, is eliminated. The performance degradation of the fuel cell and the change in time constant are inversely proportional with time; hence, by taking the inverse number of the time constant, the fuel cell degradation curve can be obtained [18]. For this process, the average lifespan should be calculated using experimental results for multiple fuel cells; however, since only one fuel cell was used in this study, the degradation curves were drawn by assuming the data measured at multiple operation points as data obtained through multiple fuel cells; the curves are presented in Fig. 10. In the seven sets of fuel cell degradation data, curve fitting was done using various mathematical models such as linear, power, logarithm, and exponential models, as these are the most widely used models; the model with the highest correlation was selected as the fuel cell degradation model. In this case, the fuel cell degradation curve obtained using the linear model had highest correlation; the time t at which the degradation curve reaches 0 indicates the time at which the fuel cell output falls to 0, leading to complete degradation. Table 4 shows the results of curve fitting of fuel cell degradation curve using the linear model and the estimated lifespan (final failure time) calculated by using the fuel cell degradation models.

If the lifespan data calculated through multiple degradation curves obtained through experiments on multiple fuel cells are

Table 4
List of coefficients for degradation equations and estimated lifespans of multiple fuel cells, as shown in Fig. 10.

Degradation plot	$y = at + b$		Lifespan [h] (time to failure)
	a	b	
A	−0.0004	5.4457	13,157
B	−0.0011	9.2883	8,473
C	−0.0017	11.5781	6,835
D	−0.0021	12.6483	6,167
E	−0.0022	12.6350	5,747
F	−0.0017	11.0791	6,703
G	−0.0014	9.6421	7,091

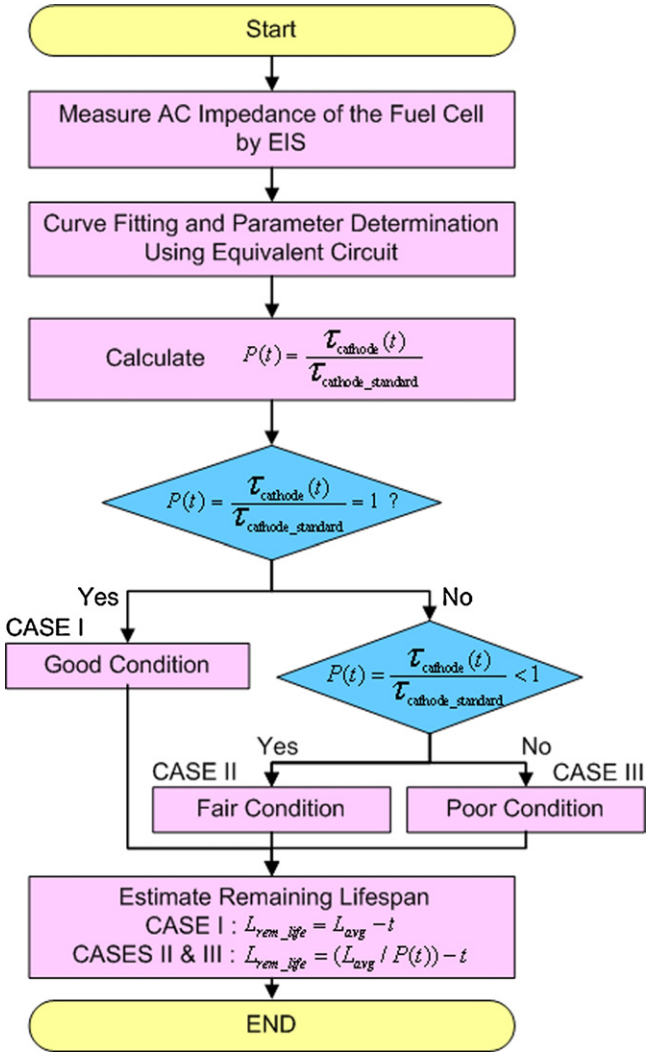

Fig. 12. Flowchart of proposed algorithm to evaluate state and remaining lifespan (L_{rem_life}) of fuel cell.

available in large quantities, the lifespan distribution and probability density function ($f(t)$) can be calculated and the reliability of a fuel cell can then be evaluated and analyzed. In this research the two-parameter Weibull distribution is used as a model for lifespan of the fuel cell because it is one of the most widely used lifespan distributions in reliability engineering and a versatile distribution that can take on the characteristics of other types of distributions, based on the value of the shape parameter, β, and the scale parameter, η, as shown in Eq. (5) [19]. Therefore, once each parameter is determined depending on the type of distribution, the average lifespan time of the fuel cell can be calculated by using Eq. (6), which is composed with a gamma function. Here, the gamma function is a generalized factorial function defined for the range of all natural numbers as expressed in Eq. (7). This process can be done by the commercial software such as Weibull++, which is used to calculate the average lifespan and provide diverse analysis functions related to reliability. This study obtained the probability density function for the fuel cell from virtual lifespan data in Table 4 using Weibull++ as shown in Fig. 11 and the distribution type used was normal distribution. In addition, the parameters for the scale and shape were 8324.54 and 4.63, respectively; the average lifespan of the fuel cell was calculated as 7609 h.

$$f(t) = \left(\frac{\beta}{\eta}\right)\left(\frac{t}{\eta}\right)^{\beta-1} \exp\left[-\left(\frac{t}{\eta}\right)^{\beta}\right] \quad (5)$$

where η is the scale parameter and β is the shape parameter.

$$E(T) = \eta\Gamma\left(1+\frac{1}{\beta}\right) \quad (6)$$

where Γ is the Gamma function.

$$\Gamma(\alpha) = \int_0^{\infty} t^{\alpha-1}e^{-t}dt \quad (7)$$

Fig. 12 shows the flowchart of the proposed algorithm for evaluating the state and calculating the remaining life ($L_{\text{rem\_life}}$) of the fuel cell in operation at a certain time.

4. Conclusion

This paper proposes a novel method for estimating the state and lifespan of a fuel cell in operation by measuring its AC impedance by EIS and calculating the time constant of the cathode. If the cathode time constant of the fuel cell in operation is continuously monitored using the proposed method, the fuel cell condition can be evaluated very accurately; therefore, this method is expected to prevent sudden premature failure of the operating fuel cell or stack, thereby reducing unnecessary service costs due to the abrupt failure and, ultimately, improving the system reliability significantly. In addition, if applied to an automated mass production process, the proposed algorithm is expected to aid the detection of defective fuel cells in the production stage itself.

Acknowledgement

This work (research) is financially supported by the Ministry of Knowledge Economy(MKE) and Korea Institute for Advancement in Technology (KIAT) through the Workforce Development Program in Strategic Technology.

References

[1] A. Iiyama, Proceedings of the 4th Annual Fuel Cells Durability & Performance 2008 Conference, 2008, pp. 25–48.
[2] A. Huth, Proceedings of the 4th Annual Fuel Cells Durability & Performance 2008 Conference, 2008, pp. 49–61.
[3] M. Ciureanu, R. Roberge, J. Phys. Chem. 105 (2001) 3531–3539.
[4] W. Merida, D.A. Harrington, J.M. Le Canut, G. McLean, J. Power Sources 161 (2006) 264–274.
[5] E. Laffly, M.-C. Pera, D. Hissel, Industrial Electronics ISIE IEEE International Symposium, 2007, pp. 180–185.
[6] K.H. Lee, K. Kwon, V. Roev, D.Y. Yoo, H. Chang, D. Seung, J. Power Sources 185 (2008) 871–875.
[7] N. Wagner, J. Appl. Electrochem. 32 (2002) 859–863.
[8] M.A. Rubio, A. Urquia, S. Dormido, J. Power Sources 171 (2007) 670–677.
[9] N. Fouquet, C. Doulet, C. Nouillant, G. Dauphin-Tanguy, B. Ould-Bouamama, J. Power Sources 159 (2006) 905–913.
[10] J.R. Macdonald, Impedance Spectroscopy: Emphasizing Solid Materials and Systems, John Wiley & Sons, Inc., 1987.
[11] X. Yuan, H. Wang, J.C. Sun, J. Zhang, Int. J. Hydrogen Energy 32 (2007) 4365–4380.
[12] K. Cooper, The 2006 Short Course in Fuel Cell Technology, 2006.
[13] S. Knights, Proceedings of the 4th Annual Fuel Cells Durability & Performance 2008 Conference Ballard Power Systems, 2008, pp. 59–78.
[14] S. Zhang, X. Yuan, H. Wang, W. Meïrida, H. Zhu, J. Shen, S. Wu, J. Zhang, Int. J. Hydrogen Energy 34 (2009) 388–404.
[15] D. Liu, S. Case, J. Power Sources 162 (2006) 521–531.
[16] Z. Xu, Z. Qi, A. Kaufman, J. Power Sources 156 (2006) 281–283.
[17] W.H. Press, S.A. Teukolsky, W.T. Vetterling, B.P. Flannery, Numerical Recipes, 3rd ed., 2007, Cambridge.
[18] N. Sammes, Fuel Cell Technology-Reaching Towards Commercialization, Springer, 2006.
[19] B.W. Weibull, Sweden, J. Appl. Mech. 18 (1951) 293–297.